SLAC-PUB-3360
June 1984
(I)

ČERENKOV RING IMAGING DETECTOR DEVELOPMENT AT SLAC*

STEPHEN H. WILLIAMS
Stanford Linear Accelerator Center
Stanford University, Stanford, California 94305

Summary

The imaging of Čerenkov light on to photosensitive detectors promises to be a powerful technique for identifying particles in colliding beam spectrometers. Toward this end two and three dimensional imaging photon detectors are being developed at SLAC. The present techniques involve photon conversion using easily ionized exotic chemicals like tetrakis-dimethyl-amino-ethylene (TMAE) in a drift and amplifying gas mixture of methane and isobutane.

Single photoelectrons from Čerenkov light are currently being drifted 20 cm and a new device under study will be used to study drifting up to 80 cm along a magnetic field. A short description of a large device currently being designed for the SLD spectrometer at the Stanford Linear Collider will be given.

Motivation

Flavor tagging in the new SLD spectrometer at the Stanford Linear Collider will be accomplished by a powerful combination of a high precision vertex detector and a Čerenkov-ring-imaging device. This will be a unique approach to the problem since the SLC machine parameters permit close installation of the vertex detector and, consequently, rather high tagging efficiency for the weak decays of heavy quarks and leptons. The final state particle identification from the Čerenkov counter together with this secondary vertex tag allows extremely clean charm and bottom signals to be obtained with high efficiency. As examples of the power of the system, the D signal in $k\pi$ and $K\pi\pi$ mass plots as derived from Z^0 decay jets using the SLD flavor tag system are shown in Figs. 1 and 2. Very clean mass peaks are observed, permitting background-free detailed studies of CP violation on cascade decay parameters. The efficiency and cleanliness of an inclusive D meson tag are summarized in Fig. 3.[1]

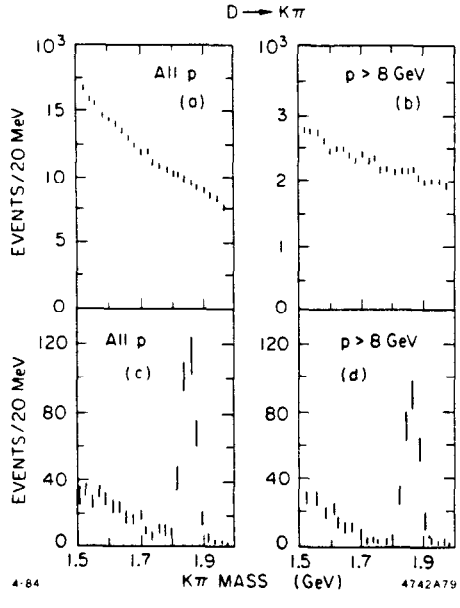

Fig. 1. The number of events versus $K\pi$ mass for two particles from the same side jets produced in Z^0 decay; (a) and (b) for all neutral charge combinations; and (c) and (d) after topology selection and particle identification in the SLD. (a) and (c) include all secondary momenta while (b) and (d) include high momenta only ($p_{tot} > 8$ GeV/c).

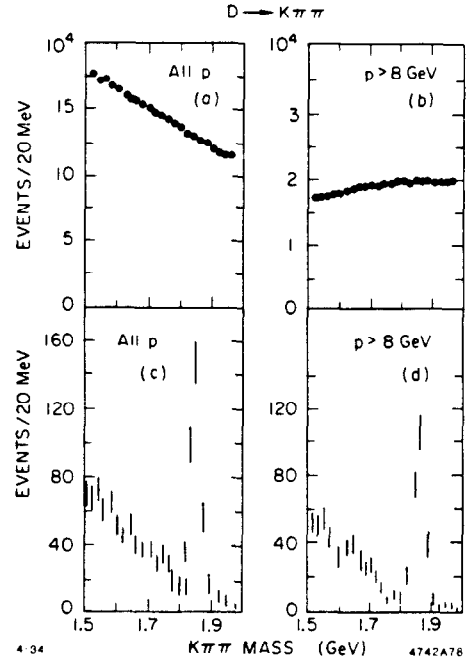

Fig. 2. The number of events versus $K\pi\pi$ mass for three particles with total charge plus or minus one from same side jets produced in Z^0 decay; (a) and (b) for all combinations; and (c) and (d) after topology and particle identification cuts in the SLD. (a) and (c) include all secondary momenta while (b) and (d) include high momenta only ($p_{tot} > 8$ GeV/c).

Other Technologies Considered

Before committing to CRIDs for the particle identification in SLD, the collaboration considered several other technologies from a performance point of view: (1) time-of-flight (TOF) with scintillators; (2) TOF with spark counters; (3) ionization

*Work supported by the Department of Energy, contract DE-AC03-76SF00515.

Invited talk presented at the 3rd International Conference on Instrumentation for Colliding Beam Physics, Novosibirsk, U.S.S.R., March 15-21, 1984

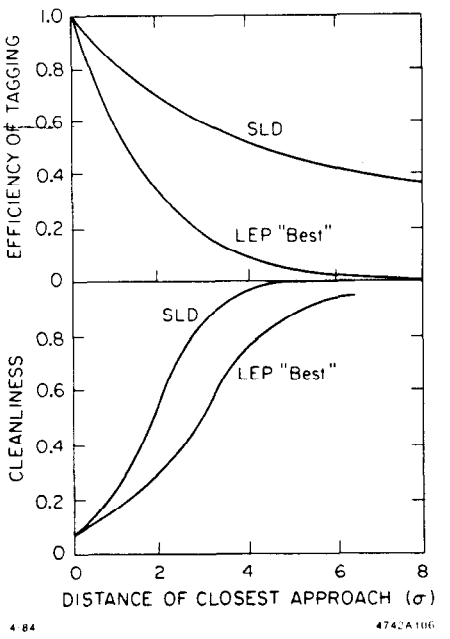

Fig. 3. (a) The fraction of D decays containing a charged K which can be tagged (efficiency) versus the number of standard deviations by which the track misses the origin for the SLD and for a "best" LEP detector. The LEP detector is assumed to have a ring imaging Čerenkov system allied to a good vertex detector, but placed much further from the interaction point, consistent with the design of the LEP machine.
(b) The fraction of identified K tracks which miss the origin by more than the given number of standard deviations which come from D decays.

from energy loss (dE/dx); and (4) threshold Čerenkov. The key factors that were brought out in discussion of their application are shown in Table I along with the advantages and disadvantages of CRID. The conclusion of the collaboration was that CRID was the most attractive alternative.

SLD CRID Design

Principle of Ring – Imaging Detectors

The principle was first put forward by Arthur Roberts[2] and recently reintroduced by the practical proposal from Ypsilantis and Seguinot.[3] It has now been adapted to several quite different experimental geometries.[4]

Table I

1. Time-of-Flight
   (a) Scintillator
      (i) Momentum range too low
      (ii) Magnetic field/phototube problem
   (b) Spark counter
      (i) Significantly better momentum range
      (ii) New technology
      (iii) Segmentation potential unclear
2. Ionization from Energy Loss (dE/dx)
      (i) Moderately good momentum range
      (ii) Ambiguous regions
      (iii) Significant change to central tracker design (pressure and gas)
3. Threshold Čerenkov
      (i) Good momentum range
      (ii) Segmentation limited
4. Ring-Imaging Čerenkov
      (i) Excellent momentum range coverage, especially with dual radiator approach
      (ii) Excellent segmentation in drift detector, even overlapping rings can be distinguished
      (iii) New technology
      (iv) Cost higher than (1), (2) and (3) but not dramatically
      (v) Robust detector, can lose performance and still be much better than (1), (2) and (3).

When Čerenkov light from a charged particle is optically focused onto a detector, the radius of the circle of Čerenkov light is a measure of the Čerenkov angle, which in turn is a measure of the velocity of the particle. The information on the velocity and the momentum of the particle permits an estimate of the particle mass. A device with gas and liquid radiators and with an ultraviolet photon detector allowing a few percent determination of the Čerenkov angle, will provide good π, K and p separation over essentially the full momentum range of SLC. Combined with the calorimetry, this also provides good lepton and hadron identification over the full momentum range.

In Fig. 4 (a), a charged particle passes perpendicularly through a thin liquid radiator producing light at approximately 45° depending on the particle velocity and the index of refraction of the liquid. If this Čerenkov light is allowed to propagate some distance before encountering the photon detector, it will form a "proximity focused" image at the detector. Light produced in the gas radiator is focused back onto the photon detector by spherical mirrors and forms a sharp image whose radius depends on the magnification of the optical system, the index of refraction of the gas, and the velocity of the particle. Using liquid (FC-72) with an index of refraction $n = 1.277$ and isobutane with $n = 1.0017$, the proximity focused circle for a relativistic particle would be around 17 cm radius and about 1.5 cm thick for the liquid, and approximately 3 cm in radius and less than 1 mm thick for the gas as shown schematically in Fig. 4 (b).

The Čerenkov photons from the charged particle of interest pass through quartz windows on the front and back of the detector box and are converted by photo-ionization of gaseous TMAE (tetrakis dimethyl amino ethylene), which has a very high quantum efficiency in the range 1700 to 2200 Å. The detector box is wound with a field cage establishing an electric drift field along the axis of the detector box, as shown in Fig. 5. The photoelectrons drift at constant velocity down the box until they arrive at the detector, which is a picket fence of

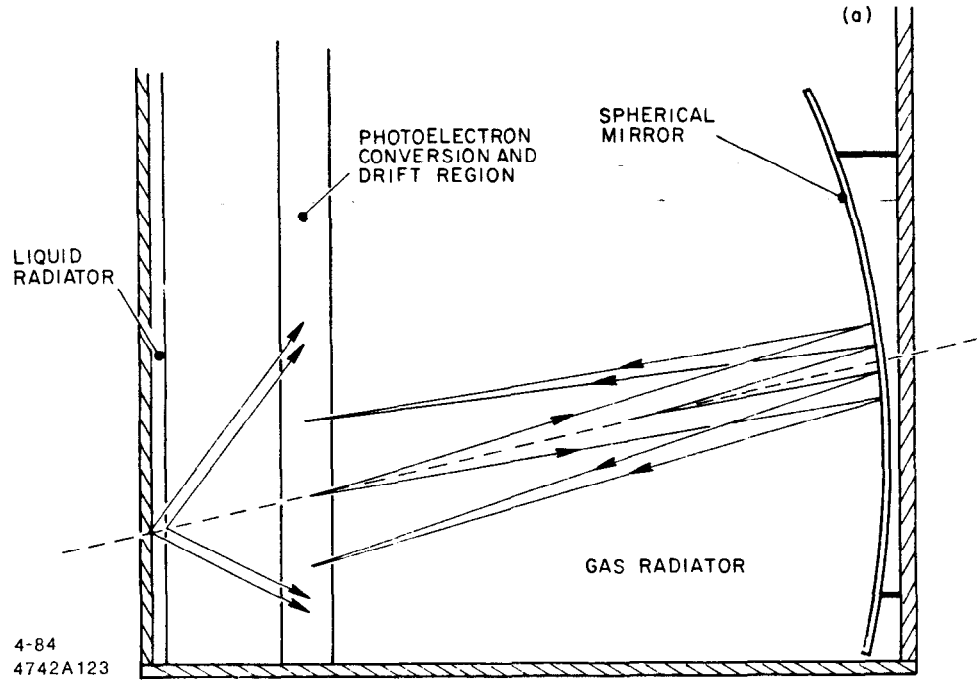

Fig. 4(a) The CRID principle for a two radiator system.

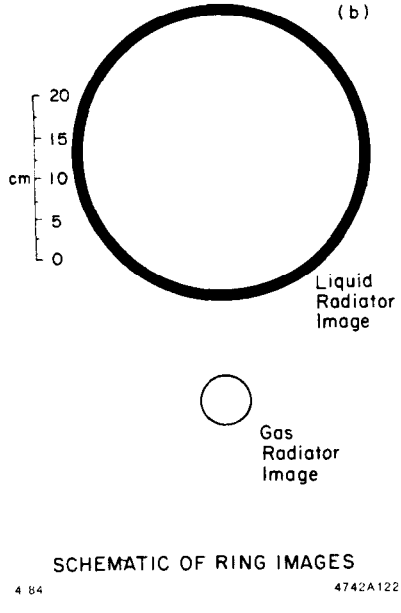

Fig. 4(b) Size of ring images produced at 90° in a liquid and gas radiator.

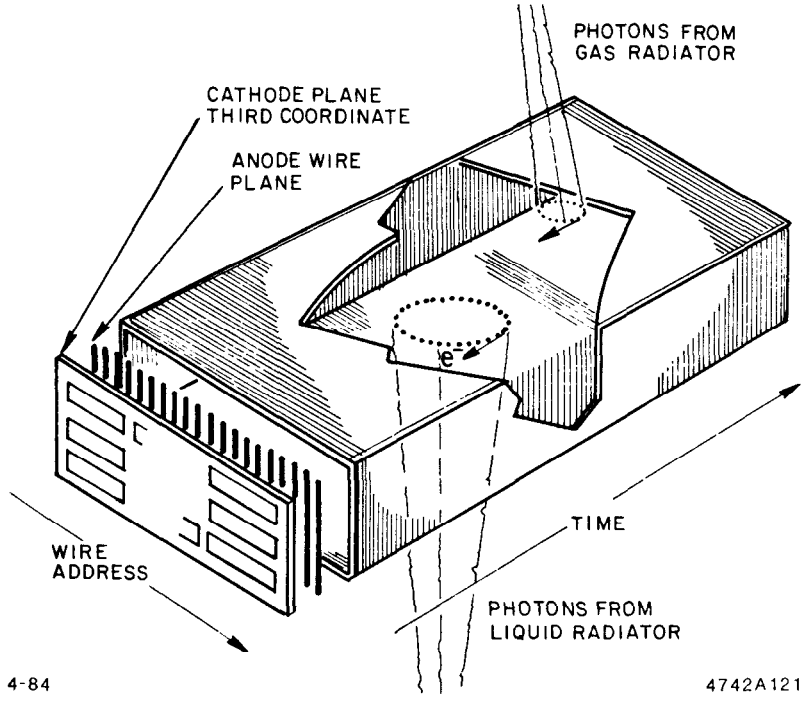

Fig. 5. Photon detector schematic.

multi-wire proportional counters. The coordinates of the point of origin of the photoelectron are recorded as the drift time of the electron and the wire address at which the electron was counted. The conversion depth which gives the parallax error comes from the third coordinate information. The Čerenkov angle for the many photons from each charged particle may, in principle, be measured to an accuracy of a few percent, allowing unambiguous identification of final state particles from below 1 GeV/c up to over 35 GeV/c.

Problems

The problems that must be solved in the design and realization of a CRID are:

(a) Minimizing all sources of aberrations of the Čerenkov circle on the detector plane;

(b) Developing a large-area, high-quantum efficiency photocathode to detect the image of the Čerenkov circle;

(c) Developing an efficient, single-electron detection system which is immune to the regenerative photon feedback background;

(d) Keeping all gases, liquids, and surfaces clean such that the far UV reflectance and transmission are maintained near their maximum value for the life of the experiment;

(e) Maintaining good control of all fields affecting the drift of the single photoelectrons;

(f) Signal processing; and

(g) Pattern recognition.

(h) The Liquid Radiator:

The choice of the material for the liquid radiator is driven by the need to have good transparency in the far ultraviolet with small chromatic dispersion and as low an index of refraction as possible. The best candidate (without using materials that require cryogenic temperature control to remain liquid) is FC-72: C_6F_{14}, perfluoro-n-hexane, with small admixtures of other isomers and some other perfluoro-paraffins. It has an index of refraction around 1.277 in the wavelength region of interest, and a rather small chromatic dispersion. The useful wavelength window for the SLD CRID is given by the absorption and transmission properties of the materials chosen; the resulting window is 1700-2300 Å as summarized in Fig. 6.[5]

The great affinity of FC-72 for absorbing gases, especially oxygen, can cause reduced UV transmission and, hence, reduced overall quantum efficiency. Thus it is essential to keep the FC-72 free of dissolved gases. The transmission of FC-72 is shown in Fig. 7 for a liquid at three different levels of cleanliness: a) spectroscopic grade C_6F_{14}, b) an FC-72 sample after passing through an Oxisorb filter, and c) an FC-72 sample left standing in a partially sealed container. The UV transmission of FC-72 can be maintained by continuously circulating the liquid through a purification system.

R&D Status at SLAC

Current Results from SLAC

The SLAC R&D effort has centered around a 20 cm drift box with a PWC picket fence at the end. The proximity focussing method has been used exclusively for generating the Čerenkov light. The radiator in use is the FC72 liquid radiator. The device is illustrated in Fig. 8.

The transparency of the freon radiator has been improved by circulating the liquid through an oxygen absorbing filter (Oxisorb) before filling the cell. Improvement in the spectral transmission in the region of interest is shown in Fig. 7. Some deterioration of the transparency in the cell occurred during the tests therefore a recirculating system is being developed.

The drift box is filled with methane (70%) and isobutane (30%). This gas combination is the best found to date for producing a reasonable pulse height spectrum from single photoelectrons. Even so the pulse spectrum becomes very broad with the increase in voltage over plateau as shown in Fig. 9.

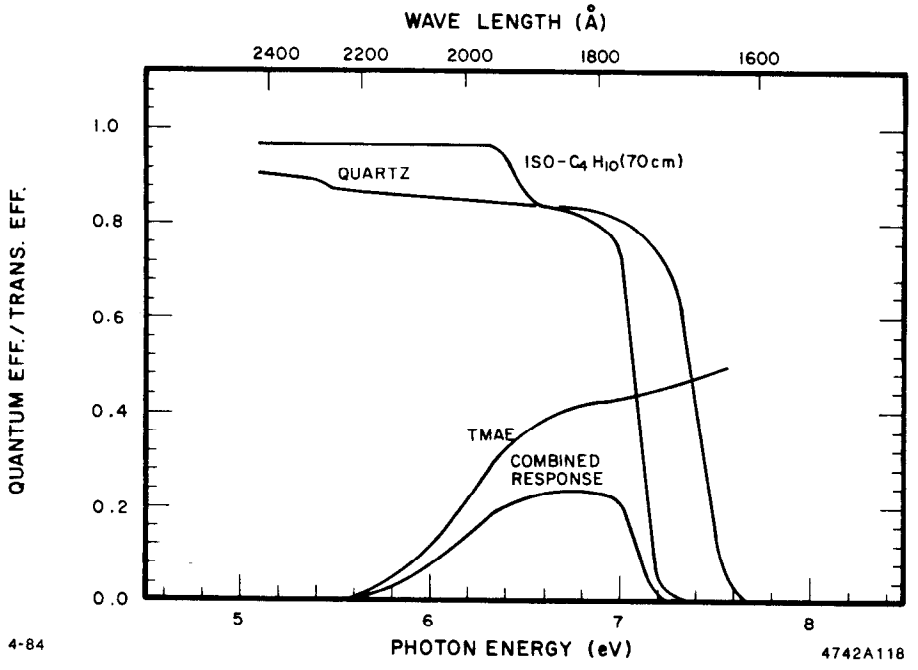

Fig. 6(a) Transmission of quartz, isobutane, and quantum efficiency of TMAE.

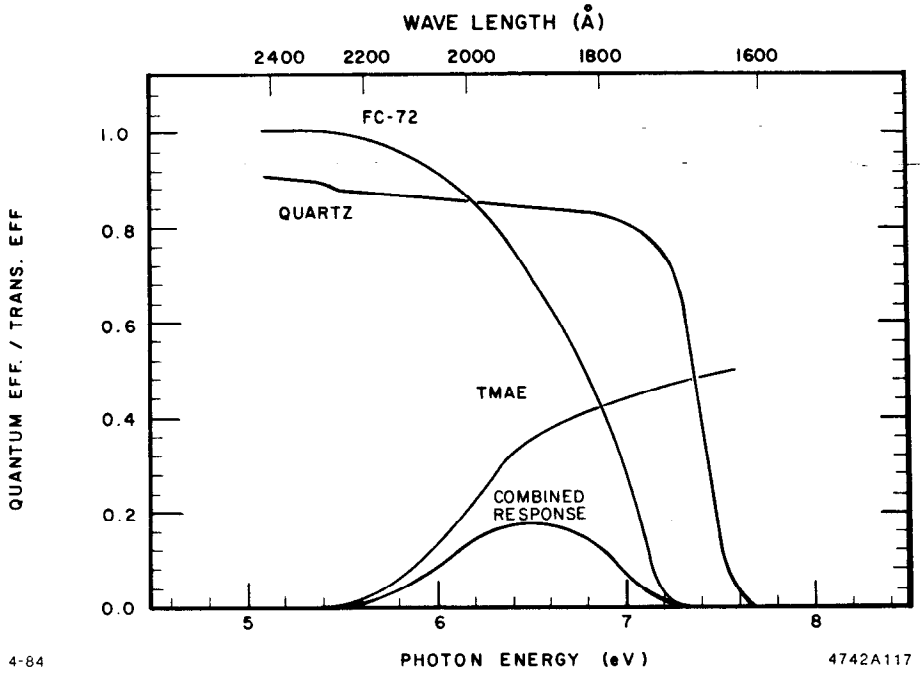

Fig. 6(b) Transmission of quartz, FC-72 and the quantum efficiency of TMAE.

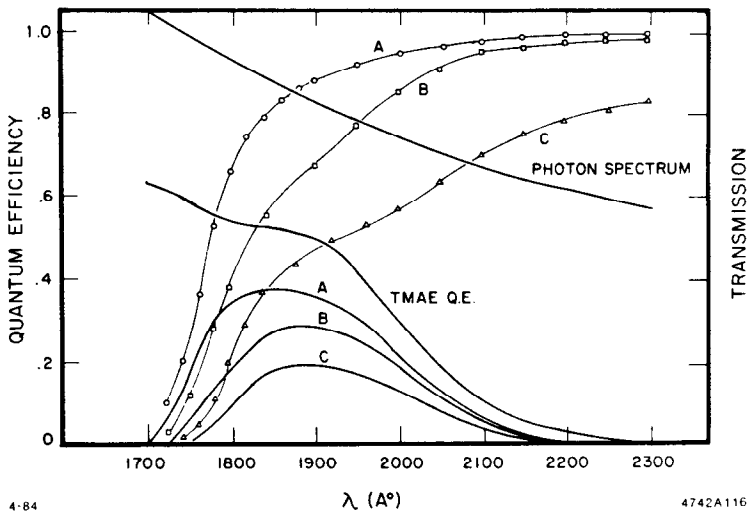

Fig. 7. Transmission of three FC-72 samples as a function of wavelength: (a) Spectroscopy grade C_6F_{14}. (b) After circulation through Oxisorb filter. (c) FC-72 after exposure to air (O_2 and H_2O, *etc.*).

The photoionizing gas, TMAE, is used by passing the methane-isobutane mixture through a bubbler at 28°C and keeping all downstream gas lines and the drift box/detector at 35°C to avoid condensation of the vapor.

Two picket fence detectors have been used to date: one is a conventional PWC with 20 μ wires spaced at 2 mm, the other consists of 20 μ wires spaced at 4 mm with solid copper blinds between each amplifying wire. UV photons produced during the gaseous amplification of ionization electrons are partially blocked from producing secondary photoelectrons. This is especially important when the primary ionization originates from the dE/dx loss due to a charged particle passing through the drift region producing hundreds of primary electrons, which drift down to the picket fence.

The electronics consisted of a low noise hybrid preamplifier attached to the amplifying wire a few centimeters from the detector. This stage was followed by 40 feet of 100 Ω coax and a 733 postamplifier. The output signals were discriminated by modified (desensitized) LeCroy PWC discriminators. A TAC with four hit capability then stored the time information until digitized by a fast scanning, microprocessor-driven ADC (called a brilliant ADC or BADC). A total of sixty-four channels with four hits each were stored in the BADC until readout through CAMAC by the FORTRAN program in the VAX.

With each event two PWC beam chambers with 1 mm wire spacing were read out. Two x and two y planes separated by 50 cm defined the tracks which were then extrapolated to the plane of the drift box. Each hit from the drift box electronics could be converted to centimeters and treated as a residual from the extrapolated beam track. Each hit was therefore an independent measurement of the ring radius on Čerenkov angle subject to the uncertainties of the proximity focussing method.

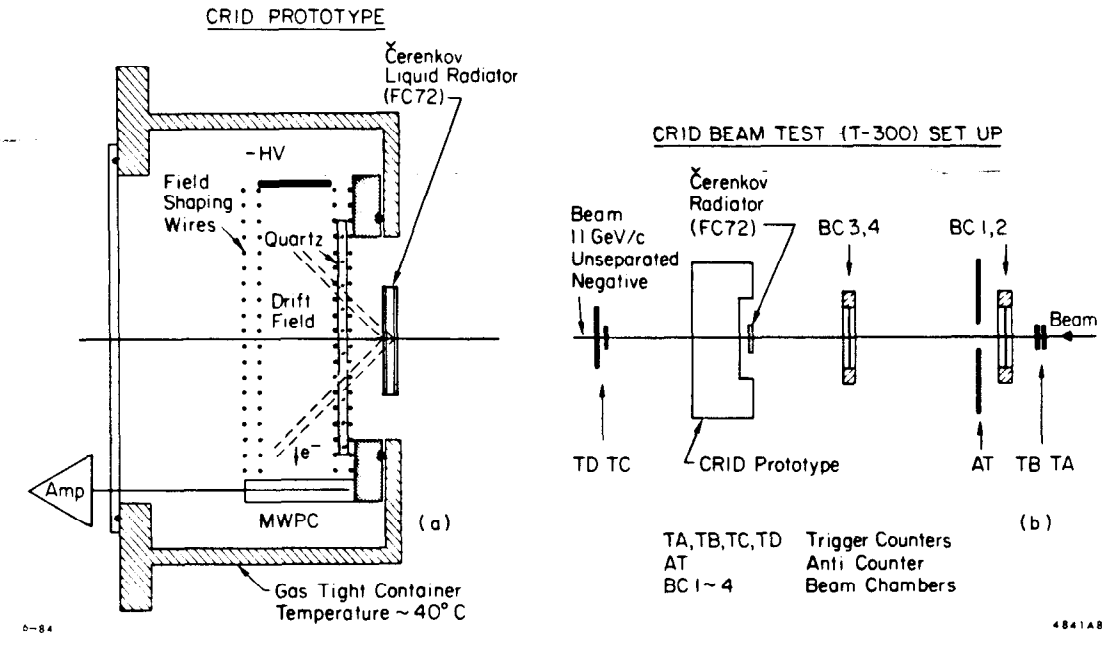

Fig. 8. (a) The drift box and Čerenkov radiation cell. (b) The drift box and beam chamber.

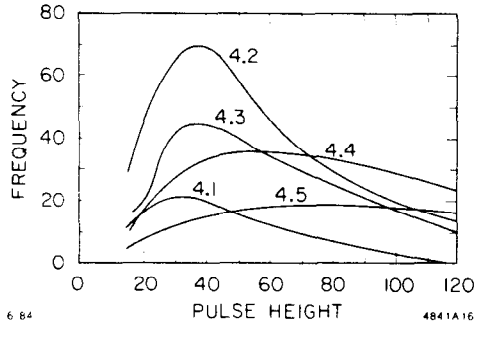

Fig. 9. Pulse height spectrum setup variation from 4.1 to 4.5 KV and the unblinded picket fence detector.

Fig. 10 shows the photoelectron residuals (x and y) in the drift region from a few hundred extrapolated beam tracks. The picket fence gain was high for this picture in order to illustrate the photon feedback which dominates the residuals after the beam ionization drifts into the picket fence.

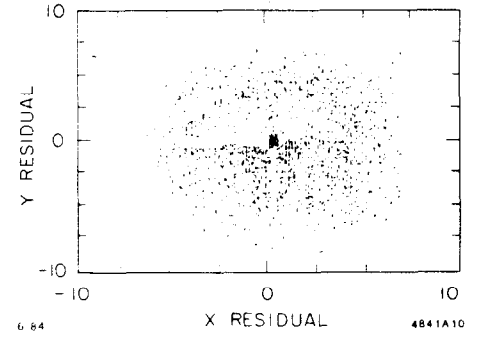

Fig. 10. x and y residuals for a few hundred beam tracks: high gain, high feed back.

Fig. 11 represents a few hundred tracks after turning the gain down to a more reasonable value, however some feedback still exists.

Fig. 12 shows a few hundred tracks using the same drift box but now employing the picket fence detector with solid

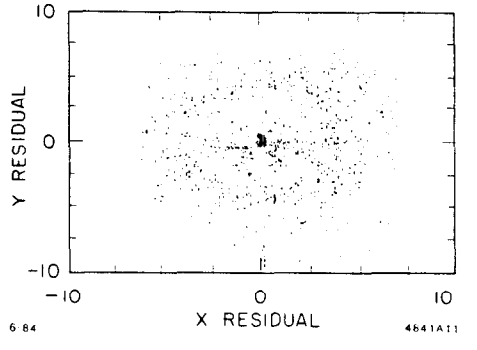

Fig. 11. x and y residuals for a few hundred beam tracks: moderate gain, moderate feedback.

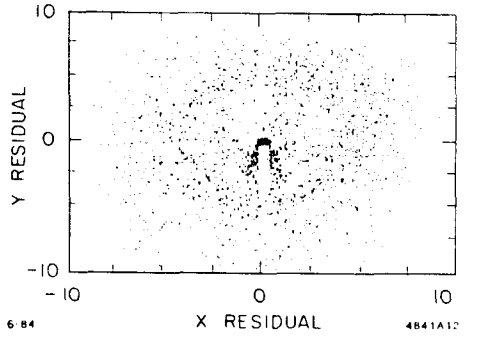

Fig. 12. x and y residuals for a few hundred beam tracks: blinded picket fence detector.

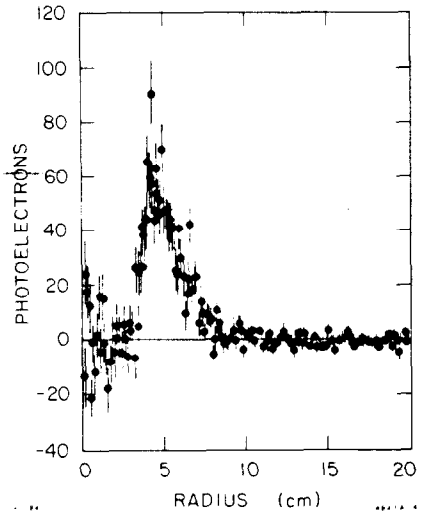

Fig. 13. Radius projection of x-y residuals for the blinded detector. Radiator-out data has been subtracted.

copper blinds between each wire to block the lateral spread of the feedback photons. There is an improvement in the feedback but more improvement is needed in order to detect very "clean" Cerenkov photon rings.

Fig. 13 illustrates in a radius plot, the strength of the Čerenkov signal relative to background for the blinded detector. Several individual events are shown in Fig. 14.

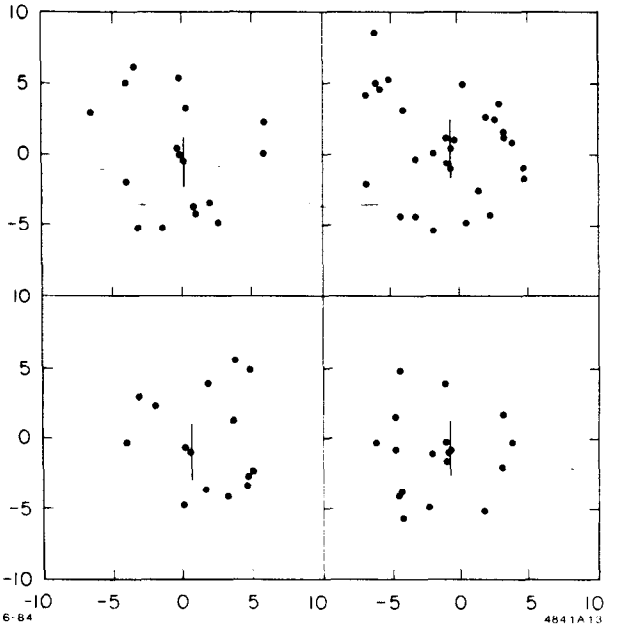

Fig. 14. Individual CerenkovRings taken with the unblinded detector operating at moderate gain.

When one counts the photoelectrons for the unblinded detector in the early time semi-circle one finds 5-8 photoelectrons per image. An average of twelve for a complete circle can be expected when the feedback is eliminated. Upon remeasuring the

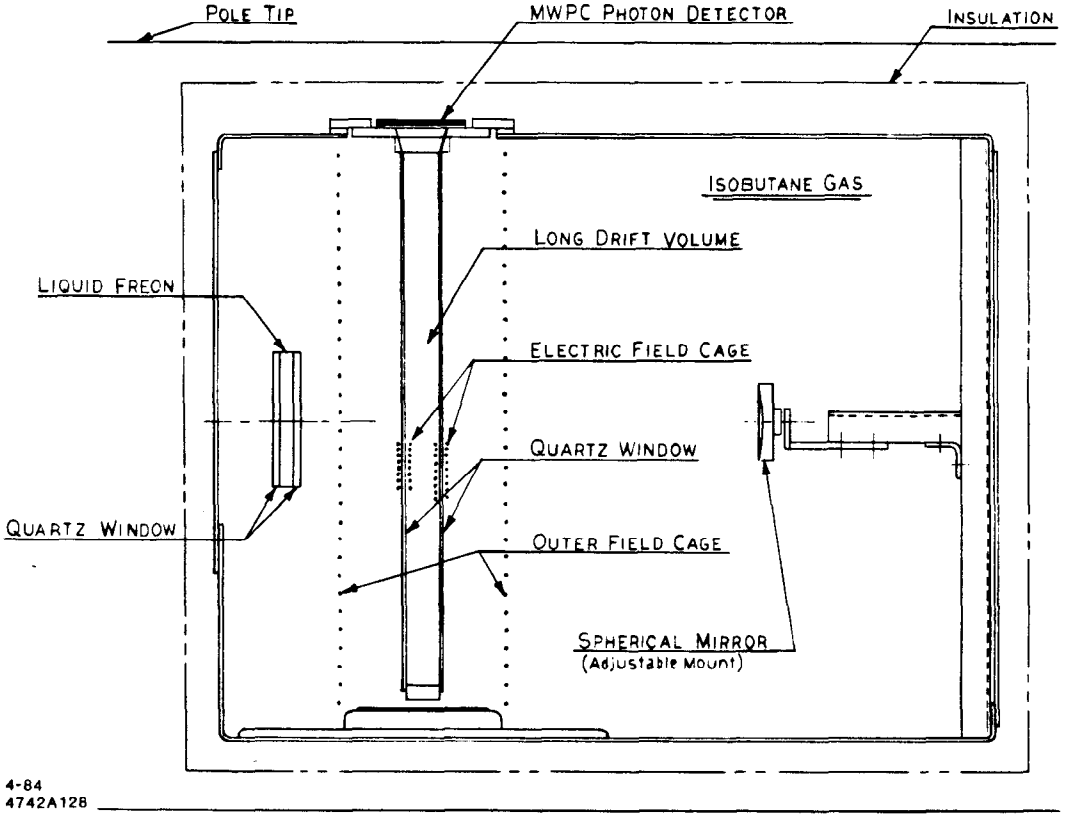

Fig. 15. Long drift with magnetic field test device.

transparency of the FC72 sample used in this data we found that it was 30% worse than the best measurements when it was recirculated through Oxisorb. Correcting for the FC72 absorption (and nothing else), we calculated an N_0 of forty-two where we expect fifty from information on TMAE quantum efficiency, quartz and FC72 transparency.

Future R&D at SLAC

The SLD CRID design requires the drifting of photoelectrons moderate distances in a magnetic field. We have therefore constructed and will soon begin tests on the 80 cm drift device show in Fig. 15. It will allow us to test the problem of drifting photoelectrons long distances and also to study the effects of a collinear magnetic field, as the box fits inside a 1 m gap dipole magnet capable of fields up to 20 kilogauss.

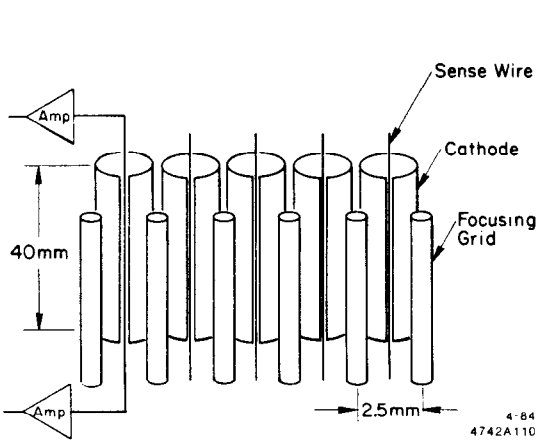

Fig. 16(a) A photon detector using slit tubes.

There is a need to readout the third coordinate in the drift box (wire number and drift time are currently readout). The uncertainly in the photon conversion depth contributes significantly to the separation capability of the SLD CRID device. Toward this end we are planning to use the device illustrated in Fig. 16. The key elements are:

1. Separation of the gain mechanism into a low-gain preamplification gap and a low-gain proportional tube;
2. Nearly complete blocking of feedback photons by the tube;
3. Reduced positive ion feedback from the tube into the drift region by the preamplification gap; and
4. Improved spatial resolution along the picket fence as a consequence of the large electron cloud emerging from the preamplification gap which enters one or two neighboring proportional tubes.

Preamplification gaps have been used in recent years,[6] especially for detecting single photons, with high gains in a variety of gases, although here we need only a modest gain of twenty-five (after transfer gap losses). The electrostatic study shown in Fig. 16 (b) indicates that collection efficiency of charge from the preamplification gap into the split tube is 100%.

SLD Design Status

Fig. 17 shows the barrel and end cap CRIDs as they are currently designed for SLD. The goal of 98% coverage is achieved by this design. The barrel region three meter central barrel detector is broken into four drift regions of 75 cm each to avoid problems of very high voltages and long drift paths. Each wire is readout at both ends so that each photoelectron is measured

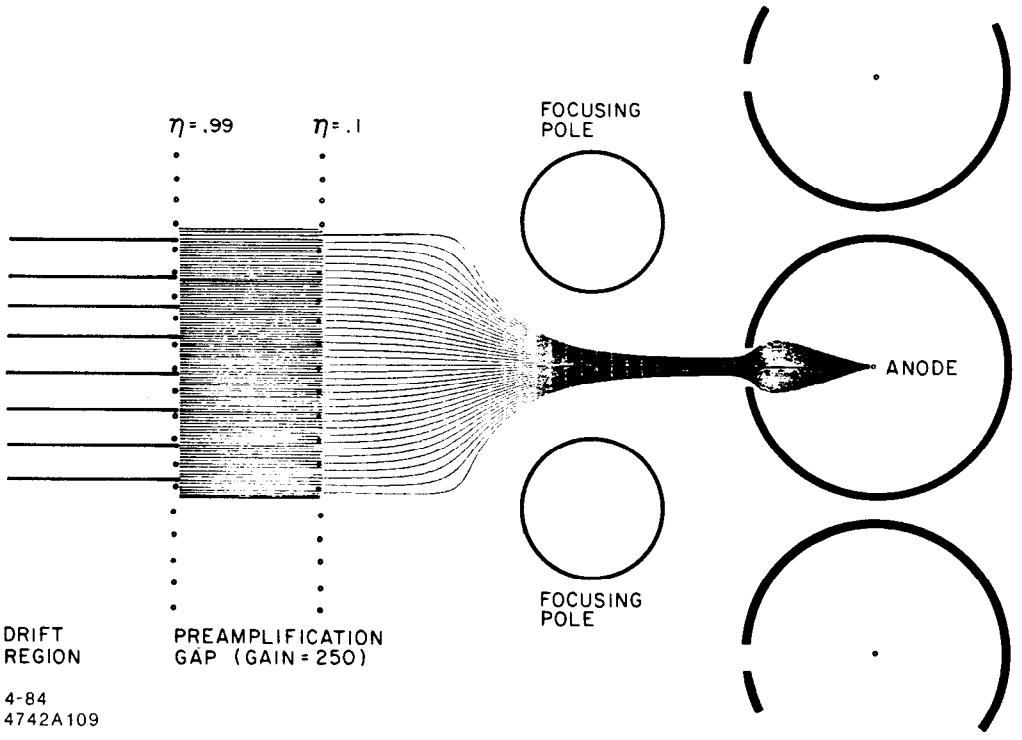

Fig. 16(b) Electrostatics of detector.

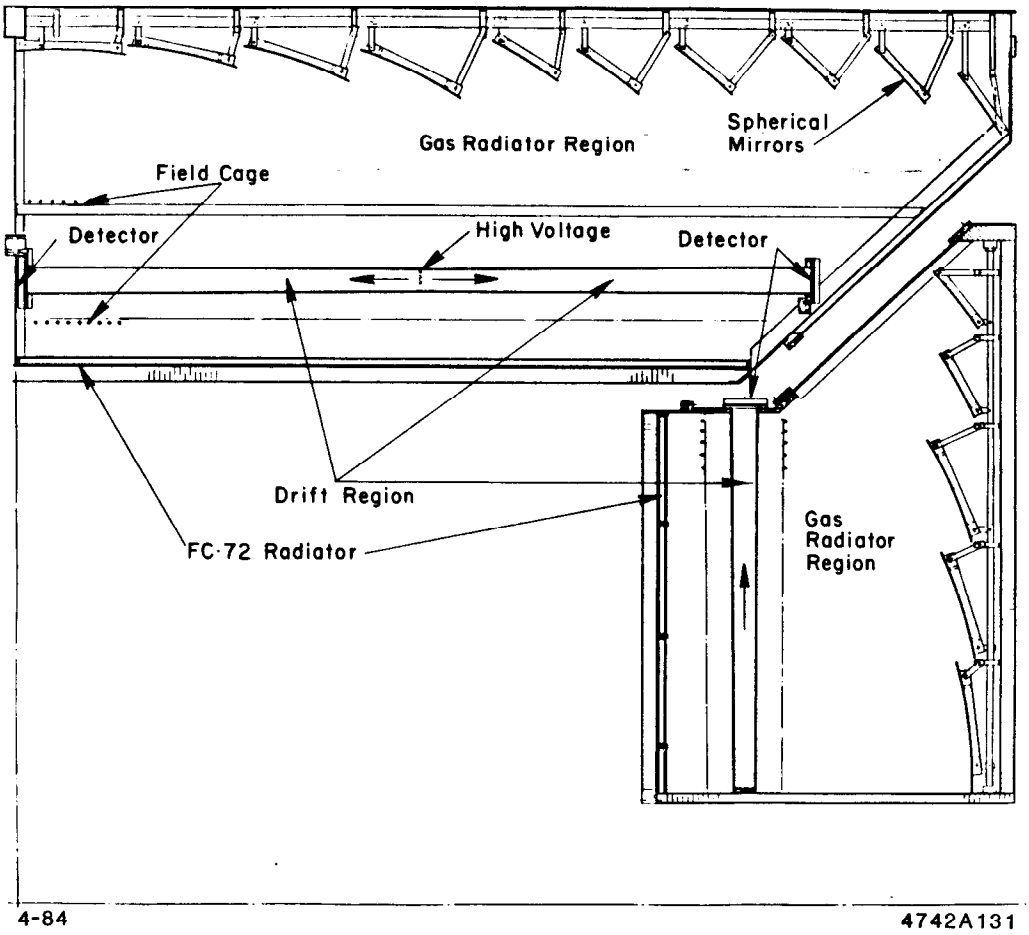

Fig. 17. Schematic of barrel and endcap longitudinal section.

in three-dimensions by use of charge division. Each end cap consists of a single volume made of twelve pie shaped drift fields. Photoelectrons drift outward at the Lorentz angle to one of the twelve detectors of the outer circumference.

The particle separation characteristics of the device are shown in Fig. 18. A study was made which demonstrated that a loss of photon detection efficiency of 50% will move the separation curves toward lower momentum by only a few GeV, leaving the device much more effective than other methods of particle separation.

Conclusion

In conclusion, particle identification still looks as though it may prove to be an important component of colliding beam spectrometers, especially when combined with a good vertex detector. Particle separation performance curves for Čerenkov-ring-imaging make it a clear choice for the physics goals. R&D results at SLAC have shown that the imaging of 10-25 photoelectrons from the particle's Čerenkov light is possible.

Acknowledgments

The work described here is being carried on by the following people: V. Ashford, F. Bird, D. Leith, S. Shapiro, B. Ratcliff, T. Shimomura and myself. In addition I would like to thank A. Nuttall, the design engineer, and R. Reif, the chief technician, for their contribution to this work.

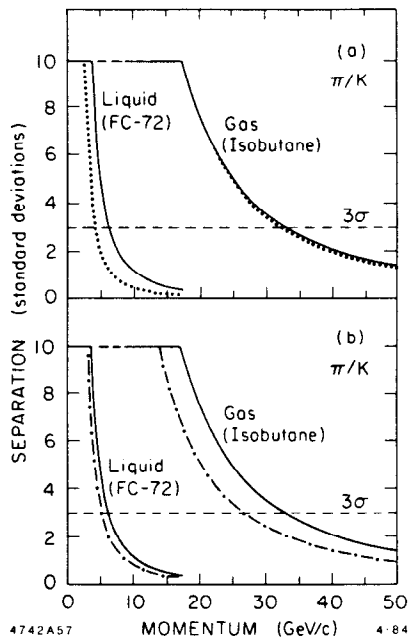

Fig. 18. Particle separation capability of the CRID system at 90° versus momentum. The performance of the liquid (FC-72) and gas (isobutane) radiators are shown separately. The curves are "saturated" at 10 σ (see text). The dashed line indicates the region where the heavier particle is below radiator threshold. The separation is shown for; a) e/π, b) π/K, and c) K/p.

References

1. B. Ratcliff, "D Meson Reconstruction at the Z^0," SLD Note No. 108.
2. A. Roberts, Nucl. Instrum. Meth. 9, 55 (1960).
3. J. Seguinot and T. Ypsilantis, Nucl. Instrum. Meth. 142, 377 (1977).
4. (a) DELPHI: CERN/LEPC/83-3, LEPC/P 2, 17 May 1983.

   (b) E-605: H. Glass *et al.*, Nucl. Sci. Symp. 1982:30 (IEEE Trans. NS – 30, No. 1, February 1983).

   (c) LOGIC: B. Barish *et al.*, CERN-LEP-LI-(6), January 1982, p. 28.

   (d) OMEGA: Bonn/Lancaster/Manchester/RAL/Sheffield. Proposal No. 231-Addendum 4, PPESP/82/24. M. Davenport *et al.*, Nucl. Sci. Symp. 1982:30 (IEEE Trans. NS – 30, No. 1, February 1983).

   (e) UA-2: RICH Collaboration (P. Baillon *et al.*), CERN/SPSC/82-55, January 1982.

   (f) SLD: R. Baltrusaitis *et al.*, SLC-LI-09, 1982, p. 59.
5. D. F. Anderson, LA-UR-80-3158.
6. G. Charpak *et al.*, Nucl. Instrum. Meth. 164, 419 (1979).